

Supercooled water in an Arctic polynya: observations and modeling

Ragnheid SKOGSETH,¹ Frank NILSEN,^{1,2} Lars H. SMEDSRUD³

¹*The University Centre in Svalbard (UNIS), PO Box 156, NO-9171 Longyearbyen, Norway
E-mail: ragnheid.skogseth@unis.no*

²*Geophysical Institute, University of Bergen, Allegaten 70, NO-5007 Bergen, Norway*

³*Bjerknes Centre for Climate Research, Allegaten 55, NO-5007 Bergen, Norway*

ABSTRACT. In situ field measurements of an active polynya in Storfjorden, Svalbard, during April 2006 are presented. A surface heat flux, estimated to be 400 W m^{-2} , produced frazil ice that was advected away from the fast ice edge during the end of a polynya event driven by cold winds from the northeast. Conductivity, temperature and depth casts from the fast ice edge of the polynya were calibrated by accompanying water samples, and reveal a supercooling event that lasted for 3 days in a 5 m deep water column. Surface salinity reached 35.9 psu from brine release during ice growth. The maximum supercooling measured was $0.037 \pm 0.005^\circ\text{C}$ below the in situ freezing point near the surface and $0.016 \pm 0.005^\circ\text{C}$ at the bottom; the mean supercooling gradient was $0.020 \pm 0.005^\circ\text{C}$ between the surface and the bottom. These measurements are consistent with results from a one-dimensional frazil ice model, confirming that such supercooling levels can be expected. Frazil ice concentrations in the water were modeled to be lower than 0.02 g L^{-1} , due to advection in the surface layer. Seven frazil/grease ice samples taken from a place where advection was blocked along the fast ice edge showed a mean salinity of 26.2 psu, indicating 25% frazil ice and 75% sea water in the grease ice. The water-column salinity decreased during the measurement period due to less saline water replacing newly formed brine-enriched shelf water flowing down to deeper parts of Storfjorden. The supercooling ceased when the wind direction turned to the east, with higher air temperatures and warmer and less saline water being pushed into Storfjorden by the northward Ekman transport. These are the first in situ observations from an active Arctic polynya with concurrent sampling of hydrography and frazil ice, and the supercooling is the maximum observed in recent years with modern and accurate instrumentation.

INTRODUCTION

Supercooled water is water in liquid state at temperatures below the freezing point referred to the surface (potentially supercooled) or the in situ freezing point (in situ supercooled). Criteria for formation of in situ supercooled water were suggested by Coachman (1966) to be (1) large net heat loss from the water and (2) transport of the supercooled water away from existing ice before crystallization can take place. Frazil ice, fine spicule, plate or discoid crystals about 1–20 mm in diameter and 1–100 μm in thickness, form in such turbulent supercooled water (Kivisild, 1970; Martin, 1981; Daly, 1984; Smedsrud, 2001). The growth efficiency and conditions for frazil ice vary with the degree of supercooling, and possibly also the form of the ice crystals (Ushio and Wakatsuchi, 1993).

In laboratory experiments maximum levels of supercooling of ~ 0.020 – 0.050°C have been found (Daly, 1984; Smedsrud, 2001). This supercooling level is created by, and varies with, the heat flux, and is limited by the growth of frazil ice. Frazil-ice growth releases latent heat and increases the water temperature. It depends on the availability of small crystals (seeding rate and secondary nucleation), and also on the level of turbulence. Within a few minutes in fresh-water laboratory experiments (Daly, 1984), or a few hours in saline water experiments (Smedsrud, 2001), the water temperature reaches an equilibrium within $\pm 0.005^\circ\text{C}$ of the freezing point. Model studies explain this temperature

behavior by assuming a small initial ice formation caused by a few tiny crystals with little ice area exposed to the supercooled water (Omstedt and Svensson, 1984). The supercooling increases until the increasing ice area and crystal concentration result in latent heat release larger than the heat flux to the cold adjacent environment. Eventually the water temperature rises towards the freezing point and reaches an equilibrium where the heat flux is balanced by the no longer limited growth of frazil crystals.

Frazil ice formation occurs in specific environments in the polar oceans. Most commonly, frazil ice forms in any region of open water at the freezing point that experiences a minimum level of turbulence and a significant heat flux to the atmosphere. Frazil ice also forms adjacent to ice shelves and icebergs, at the interface between two layers with different salinities and at their freezing point, and from the drainage of brine from sea ice (Martin, 1981). Decreasing freezing-point temperature with depth ($7.53 \times 10^{-4}^\circ\text{C m}^{-1}$; Millero, 1978) causes large supercooling beneath Antarctic ice shelves and Arctic icebergs (Lewis and Perkin, 1983, 1986). This mechanism, melting of ice at depth and refreezing in shallower water, is often referred to as an ice pump, and may control topographic features of the ice bottom (Untersteiner and Sommerfeld, 1964). The ice pump is commonly observed beneath both the Filchner–Ronne Ice Shelf, Antarctica, (Lusquiños, 1963; Orheim and others, 1990; Khazendar and Jenkins, 2003; Nicholls and others, 2004) and the Ross Ice Shelf, Antarctica, (Littlepage, 1965;

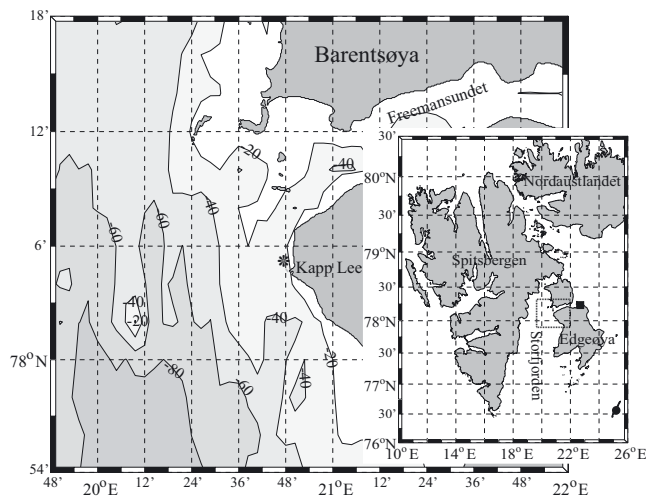


Fig. 1. Storfjorden in the Svalbard archipelago, with Kapp Lee indicated. The location of the repeated conductivity, temperature and depth (CTD) profiles is marked with a black star. The boxed area within the inset indicates the borders of the larger map. The meteorological stations are indicated with a black circle (Hopen island) and a black square (Edgeøya) in the small map. Bathymetry contour spacing is 20 m.

Countryman, 1970; Leonard and others, 2006) with in situ supercooling down to $\sim 0.060^{\circ}\text{C}$ (Lusquiños, 1963) and 0.035°C (Nicholls and others, 2004).

Supercooled water has only been observed briefly in the Arctic. Previously the expected degree of Arctic supercooling has been $0.010\text{--}0.001^{\circ}\text{C}$, but direct determination of the freezing point of sea water, in situ, has been experimentally difficult in the past (Untersteiner and Sommerfeld, 1964). This is because (1) supercooling probably occurs in places where it is difficult to measure, (2) supercooling levels are small and close to instrument uncertainties and (3) supercooling drives ice formation that may disturb measurements. Coachman (1966) presents a review of reported supercooling in the polar regions. He reports supercooling down to 0.130°C in the surface layer of the Eurasian Basin and also potential supercooling down to 0.020°C throughout the winter in the surface layer of the Canada Basin, determined by the drifting ice station, Arlis-I.

Instruments and determination of the freezing point have improved since the 1960s. Supercooled water due to surface cooling in leads and polynyas has been observed north of Svalbard with potential supercooling down to 0.008°C (Lewis and Perkin, 1983), in the St Lawrence Island (Alaska, USA) polynya with in situ supercooling $<0.010^{\circ}\text{C}$ (Drucker and others, 2003), and in the northwestern polynya of the Okhotsk Sea with potential supercooling down to 0.007°C (Shcherbina and others, 2004), the latter two with moorings during wintertime. Mooring observations with upward-looking sonar (Drucker and others, 2003) and a downward-looking acoustic Doppler current profiler (Leonard and others, 2006) reveal significant correlations between the presence of supercooled water and frazil ice.

A recurrent Arctic coastal polynya in Storfjorden, Svalbard (Fig. 1) is known to form substantial amounts of frazil ice (Haarpaintner and others, 2001; Skogseth and others, 2004, 2005a), but no previous observations of supercooled water are reported for this area. Here we present new hydrographical observations of in situ supercooling reaching

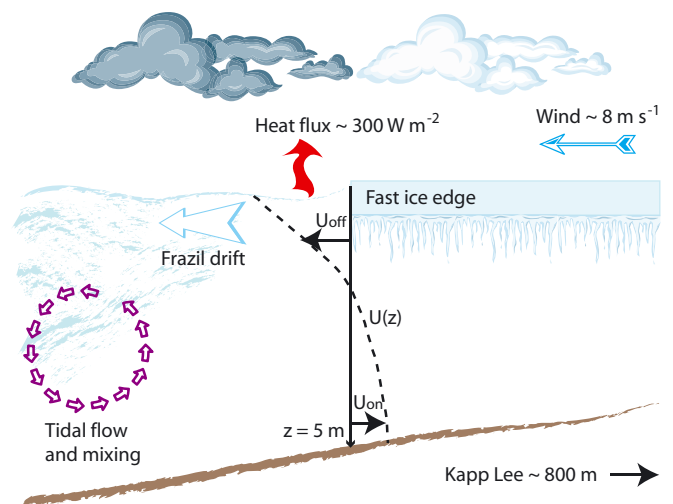


Fig. 2. A sketch of the conditions at the field site during the experiments. Profiles were made repeatedly in the 5 m water column from the fast ice edge, ~ 800 m from Kapp Lee on Edgeøya at the upwind side of the Storfjorden polynya. The wind was directed off the fast ice edge with speeds $\sim 8\text{ m s}^{-1}$. The surface water and frazil ice along the fast ice edge were advected into the polynya with a modeled speed $U_{\text{off}} \sim 6\text{ cm s}^{-1}$, setting up a returning flow modeled to be $U_{\text{on}} \sim 2\text{ cm s}^{-1}$ close to bottom. Frazil ice was not visible at the measuring site, which is supported by a very small modeled frazil ice concentration of $\sim 0.01\text{ g L}^{-1}$ (see Fig. 7).

0.037°C that lasted for several days under cold northeasterly winds in the Storfjorden polynya. To our knowledge, this is the first high-accuracy in situ hydrographical sampling of supercooled water in an active polynya with frazil ice formation.

In this paper, we discuss the processes taking place at the upwind side of the Storfjorden polynya. The in situ measurements are compared with results from a numerical model describing the heat loss, vertical mixing processes, resulting supercooling and frazil ice formation. Through this we evaluate to what extent the situation we sampled was peculiar, as suggested by the 'record' of the in situ supercooling, or whether the situation is illustrative of the general situation at the upwind side of any wind-driven coastal polynya. If this is a general process, it is largely under-sampled, and our measurements should be of general interest within the fields of sea ice and polar oceanography.

DATA AND METHOD

Field site

The experiments were performed close to Kapp Lee (Fig. 1) on the fast ice edge at the upwind side of the Storfjorden polynya. The wind was directed off the fast ice edge towards the open water in the polynya. No snow flux was visible during the experiments. Frazil ice was not visible in the surface at the measuring site, but drifted instead along the fast ice edge into the polynya area towards the consolidated thin ice. In the shallow polynya area, mixing due to wind and tides is very effective (Skogseth and others, 2007), making the polynya water close to homogeneous. However, the ice drift during the experiments seemed to be controlled by the strong wind, whereas the tide probably had an insignificant influence. Figure 2 indicates the conditions at the field site.

Hydrography

Repeated conductivity, temperature and depth (CTD) profiles (Table 1) close to Kapp Lee on Edgeøya (Fig. 1) were obtained using a SeaBird Electronics SBE19 (unpumped) sonde and are subsets of data gathered from 31 March to 7 April 2006 (Skogseth and others, 2008). The sensors were lowered and heaved at a speed range of $0.3\text{--}1.0\text{ m s}^{-1}$ through a hole in the fast ice on 31 March and until 1500 h on 1 April (hereinafter referred to as location FI), and in open water in the polynya from the fast ice edge from 1510 h on 1 April to 5 April (hereinafter referred to as location PY). The distance between the two CTD locations was $\sim 100\text{ m}$.

To avoid freezing of the CTD sensors between stations, the CTD was kept in a heated box together with Niskin water-sample bottles. When profiling, the CTD was first lowered to 5 m depth in an area with apparently no snowdrift or frazil ice, until measurements stabilized at recognizable values, indicating no significant ice in the conductivity sensor. In total, 46 down- and upcast profiles (listed in Table 1) were obtained from 31 March to 5 April 2006 at the location indicated in Figure 1.

The temperature and conductivity sensors were aligned in advance of pressure according to the descent rates. The accuracy is 0.14 dbar for the pressure sensor, 0.005°C for the temperature sensor and 0.0005 S m^{-1} for the conductivity sensor. Calibration of the CTD data was performed using 11 water samples taken during the fieldwork with a 1.7 L Niskin bottle. During the supercooling event, surface water samples were carefully collected, using a plastic sieve to avoid introducing any frazil crystals into the bottles. SeaBird Electronics performed pre- and post-calibration routines on the CTD sensors. The uncertainty of the CTD salinities and temperatures after calibration are typically 0.01 psu and 0.005°C .

As part of the data analysis, SeaBird Electronics performed quality control on the CTD raw data. This indicated insignificant ice volume inside the conductivity sensor. Ice crystals larger than $\sim 5\text{ mm}$ could not enter the conductivity sensor, and smaller ice crystals between $\sim 100\text{ }\mu\text{m}$ and $\sim 5\text{ mm}$ would have created spikes in the raw data, which were not detected. Frazil crystals smaller than $\sim 100\text{ }\mu\text{m}$ could cause a permanent reduction in conductivity.

No current-meter data are available from the field experiment, precluding any analysis of tidal influence. Current-meter data from 2004 indicate strong tidal currents up to 53 cm s^{-1} with a half-day periodicity (Skogseth and others, 2008).

Meteorology

In situ meteorological data from Hopen and Edgeøya (Fig. 1) were provided by the Norwegian Meteorological Institute. Wind speed and direction, cloud cover and relative humidity on Hopen, and air temperature on Edgeøya were used to calculate the net heat flux from the open water to the atmosphere in the polynya (for details see Haarpaintner and others, 2001; Skogseth and others, 2004).

Supercooling

The water is supercooled when the temperature is less than the freezing point, $T - T_{\text{fr}} < 0$. The freezing-point temperature is estimated from the salinity, S , and pressure, P , following the UNESCO algorithm

$$T_{\text{fr}} = aS + bS^{3/2} + cS^2 + dP, \quad (1)$$

Table 1. CTD profiles taken under the fast ice (location FI) and from the fast ice edge into the polynya (location PY) close to Kapp Lee between 31 March and 5 April 2006

Cast	Location	Date	Time h:min:s
1	FI	31 March	14:10:45
2–5	FI	1 April	14:21:11–14:21:30
6–13	FI	1 April	14:25:10–14:25:45
14–17	PY	1 April	15:10:37–15:10:53
18–25	PY	1 April	15:12:37–15:13:08
26	PY	2 April	19:35:24
27–31	PY	4 April	16:12:49–16:13:33
32–36	PY	4 April	16:14:25–16:14:45
37–46	PY	5 April	15:06:16–15:10:23

given by Fofonoff and Millard (1983). Here, the constants are $a = -0.0575$, $b = 1.710523 \times 10^{-3}$, $c = -2.154996 \times 10^{-4}$ and $d = -7.53 \times 10^{-4}$. T_{fr} is referred to the surface when $P = 0$.

Frazil ice model

The one-dimensional model applied to the supercooling process is 'Frasemo' (frazil and sediment model) which is a vertical model that describes the state of a water column with time, as a result of surface forcing (wind, snow and air temperature). It was developed by Sherwood (2000), and frazil ice dynamics were added by Smedsrud (2002), who also validated the model using laboratory experiments.

Frasemo solves for water salinity, temperature and density, as well as vertical eddy viscosity. We used a time-step of 2 s, a vertical resolution of 0.2 m over a 5 m depth and only the frazil ice part of the model (sediment processes were ignored). Table 2 gives the relevant forcing, parameters and results. The model set-up is identical to that of Smedsrud (2002), apart from the differences described in the text.

The model was run for 24 hours using the observed air temperature on Edgeøya (Table 2) and calculated net heat flux close to that of Figure 5b. Applying an off-coast surface wind stress makes it possible to calculate alongshore and on- or offshore currents. As illustrated in Figure 2, wind forcing from Hopen island (Fig. 1; Table 2) created an offshore current (U_{off}) between the surface and 2.0 m depth, defining an upper layer. A lower layer formed between 2.0 and 5.0 m depth with a compensating onshore current (U_{on}) that balanced the offshore transport. Calculated current speeds were moderate, with $\sim 1\text{ cm s}^{-1}$ alongshore, $U_{\text{off}} \sim 6\text{ cm s}^{-1}$ at the surface, and $U_{\text{on}} \sim 2\text{ cm s}^{-1}$ at the bottom (not shown). Frazil crystals were advected away from the fast ice edge (offshore) in the upper layer, whereas no in- or outflow of frazil ice crystals was applied in the lower layer. Snowdrift (precipitation; Table 2) was divided equally over the five frazil size classes, but a sensitivity study of this parameter was performed, as it is challenging to estimate.

The initial salinity profile was the salinity measured in cast 2 on 1 April (Table 1), ~ 35.5 psu. The temperature was set to the freezing point for this salinity (-1.95°C), and integration started at midnight, making model results after 15 hours comparable to CTD casts 2–25 on 1 April (Table 1; Figs 5d and 6).

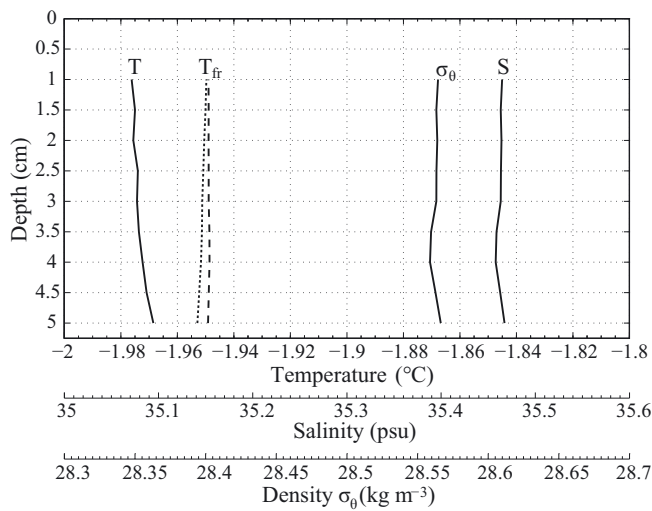


Fig. 3. Salinity, S , density, $\sigma_\theta = \rho_\theta - 1000 \text{ kg m}^{-3}$ (where ρ_θ is potential density of sea water based on the potential temperature θ), and temperature, T , vs depth in the polynya from a single representative cast on 1 April 2006 at location PY. The freezing point, T_{fr} , is shown with dotted (in situ) and dashed (referred to surface) lines.

RESULTS

Observations

A single representative CTD profile taken at location PY is shown in Figure 3. The 5 m deep water column is nearly homogeneous and in situ supercooled. However, the temperature increases slightly with depth, as expected for upward heat flux, and the salinity decreases with depth in the upper 4 m, as expected for downward salt flux. In the lower, 1.5 m deep, layer the salinity increases with depth, indicating the appearance of a bottom boundary layer.

The temperature–salinity diagram in Figure 4 shows the 5 m deep water column changing from being saline and supercooled, between 31 March and 2 April, to warmer

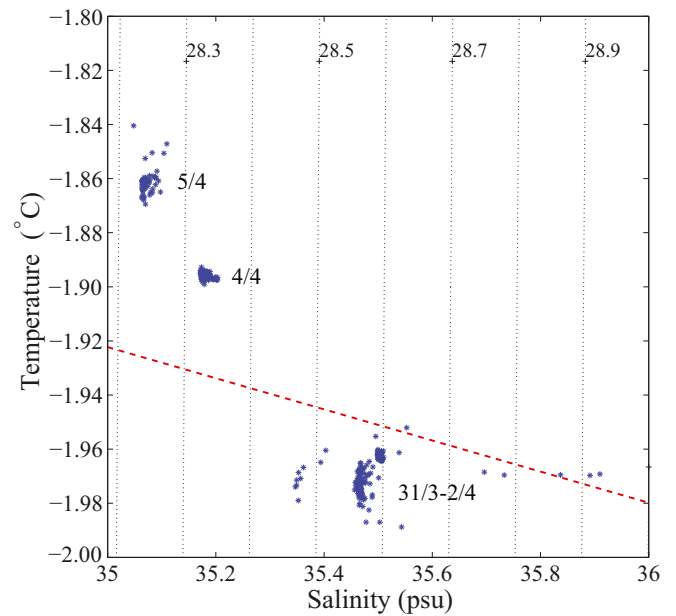


Fig. 4. Temperature vs salinity plot of the repeated CTD profiles in Storjorden outside Kapp Lee (Fig. 1) from 31 March (31/3) to 5 April (5/4) 2006. Density ($\sigma_\theta = \rho_\theta - 1000 \text{ kg m}^{-3}$) lines are drawn every 0.1 kg m^{-3} , and the freezing-point temperature referred to the surface is indicated by the dashed line.

and less saline (above freezing point) on 4 and 5 April. The salinity reaches 35.9 psu close to the surface on 31 March. The water mass in the polynya is gradually replaced by warmer, less saline and less dense water during the measuring period.

In the first part of the measurement period, the wind on Hopen was northeasterly with a speed around 8 m s^{-1} until 0100 h on 2 April. Then it turned more easterly and increased in strength (Fig. 5a). The net heat flux decreased from a maximum of 400 W m^{-2} towards zero in the same period, following the increase in air temperature from

Table 2. Summary of values relevant for the modeling of frazil ice and supercooling. All model runs use the Mellor–Yamada 2.5 turbulence closure model (Mellor and Yamada, 1982) and a five size-class distribution of frazil ice crystals

	Variable/parameter	Range	Mean	Units
Model forcing	Air temperature	−6.7, −16.7	−10.9	°C
	Wind speed	6, 10	8	m s^{-1}
	Snowdrift		0.07	mm d^{-1}
	Fetch		100	m
Key model parameters	Frazil diameter	0.025, 15	5.1	mm
	Frazil rise velocity	0.002, 28.452	9.58	mm s^{-1}
	Thermal conductivity of sea water		0.564	$\text{W m}^{-1} \text{ } ^\circ\text{C}^{-1}$
	Frazil ice density		920	kg m^{-3}
	Heat capacity of water		3989	$\text{J kg}^{-1} \text{ } ^\circ\text{C}^{-1}$
	Latent heat for ice freezing		3.35×10^5	J kg^{-1}
Relevant results	Heat flux	111, 286	183	W m^{-2}
	Ice formation rate	28.8, 74.1	47.2	$\text{kg m}^{-2} \text{ d}^{-1}$
	Ice concentration	0, 0.0248	0.0071	g L^{-1}
	Supercooling	0, −0.0450	−0.0223	°C
	Salinity increase	0.16, 0.45	0.28	psu d^{-1}
	Eddy viscosity	$1\text{--}8 \times 10^{-3}$	3.2×10^{-3}	$\text{m}^2 \text{ s}^{-1}$
	Turbulent kinetic energy	$2\text{--}25 \times 10^{-3}$	11.8×10^{-3}	m s^{-1}

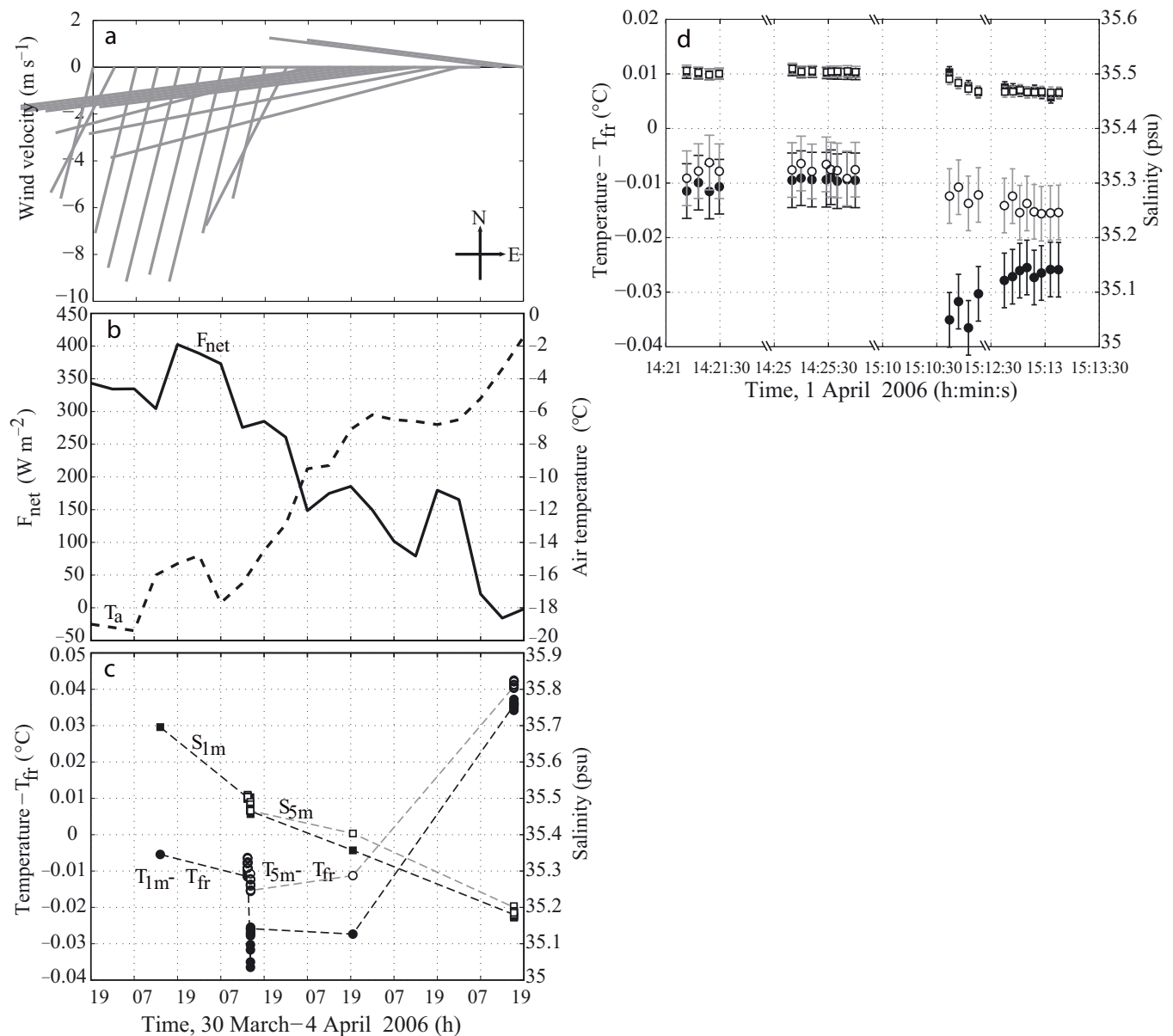


Fig. 5. (a) Stick plot of wind on Hopen island every 6 hours from 30 March to 4 April 2006. (b) Estimated net heat flux, F_{net} , from open water to atmosphere in the Storfjorden polynya and air temperature on Edgeøya, T_a , every 6 hours from 30 March to 4 April 2006. (c) Temperature relative to in situ freezing-point temperature (circles) at 1 m ($T_{1\text{m}} - T_{\text{fr}}$; black) and 5 m ($T_{5\text{m}} - T_{\text{fr}}$; white) and salinity (squares) at 1 m ($S_{1\text{m}}$; black) and 5 m ($S_{5\text{m}}$; white) from the repeated CTD profile outside Kapp Lee (Fig. 1) from 30 March to 4 April 2006. (d) As (c) for the four time-frames on 1 April 2006. The error bars are $\pm 0.005^\circ\text{C}$ and ± 0.01 psu for temperature and salinity, respectively.

-20°C towards 0°C (Fig. 5b). At the same time, the salinity and supercooling of the polynya water decreased from, respectively, 35.7 psu and $0.037 \pm 0.005^\circ\text{C}$ towards 35.2 psu and $0.040 \pm 0.005^\circ\text{C}$ above the freezing point (Fig. 5c). The supercooling and salinity at 1 and 5 m depths from the profiles obtained on 1 April are shown in Figure 5d. The supercooling is always larger at the surface, but the difference between bottom and surface is most enhanced at location PY. This is also evident in Figure 6, where the CTD profiles obtained at location FI show that temperature, salinity and hence supercooling are more homogeneous with depth under the fast ice. At location PY in open water, the supercooling increased towards the surface due to a larger heat flux. We are therefore confident that the CTD sensors worked properly and measured real supercooling and effects of freezing processes during the polynya event.

Model results

The frazil profile in Figure 7 indicates a balance of several processes. New crystals of all sizes ($25\ \mu\text{m}$ to $1.5\ \text{cm}$) are added by the drifting snow at the surface. Small crystals grow faster than larger crystals at the same level of supercooling, and the crystal growth continues until a maximum size is reached. As crystals grow larger, they become more buoyant and tend to concentrate near the surface, where they are advected out of the 2 m surface layer. Collisions between crystals produce new crystals of the smallest size, but the small crystals quickly grow into the next size class, which explains the low concentrations in Figure 7. Therefore, the medium-sized crystals contribute most to the total frazil ice concentration. The maximum total frazil ice concentration reaches $0.012\ \text{g L}^{-1}$ at the surface, and a second maximum is evident at 2.5 m depth with

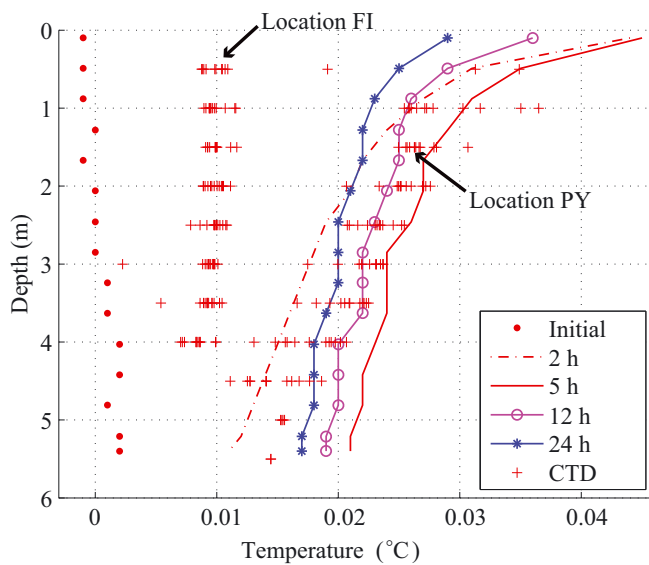


Fig. 6. Supercooling of the 5 m water column on 1 April. Model results are compared to observed supercooling (CTD) under fast ice (location FI) and in the polynya (location PY). The model is initiated at the in situ freezing point at 0000 h on 1 April, using the observed salinity (initial). Observed supercooling is nearly homogeneous with depth under fast ice and increases towards the surface in the open water at the upwind side of the polynya.

a concentration of 0.008 g L^{-1} . The secondary maximum exists because the frazil concentration at 2.5 m depth is only balanced by downward diffusion and buoyant rise, and is not limited by advection as in the surface layer. The frazil concentration is lowest at the bottom as expected.

Figure 6 shows the supercooling evolving over time through the 24 hour model run, starting at the in situ freezing point. The largest supercooling occurs between 2 and 5 hours, i.e. early in the frazil formation process, when it is similar to the maximum level measured by the CTD. When the frazil growth and advection have reached steady state, the supercooling level falls to 0.030°C at the surface and to 0.018°C at 5 m depth. The mean observed supercooling gradient at location PY compares well with the model results at ~ 15 hours. The observed supercooling at location FI is smaller and more homogeneous with depth.

DISCUSSION

Supercooling and circulation

The 5 m supercooled water column was nearly homogeneous (Fig. 3). Pronounced wind and tidal mixing are modeled in the shallow polynya area (Skogseth and others, 2007) and are probably the main reason for the observed homogeneous water column. The first part of the field period had strong surface cooling, with ice freezing and accompanying brine release, resulting in an unstable water column. Consecutive convection replaced cold and saline water at the surface with slightly less saline and cold water from below. In the shallow polynya area, convection reached the bottom. Convection of unstable supercooled surface water and accompanying underwater frazil ice production and brine release were observed by Ushio and Wakatsuchi (1993) in a laboratory study. In this way, convection driven by thermal forcing, in addition to wind and tidal mixing, are

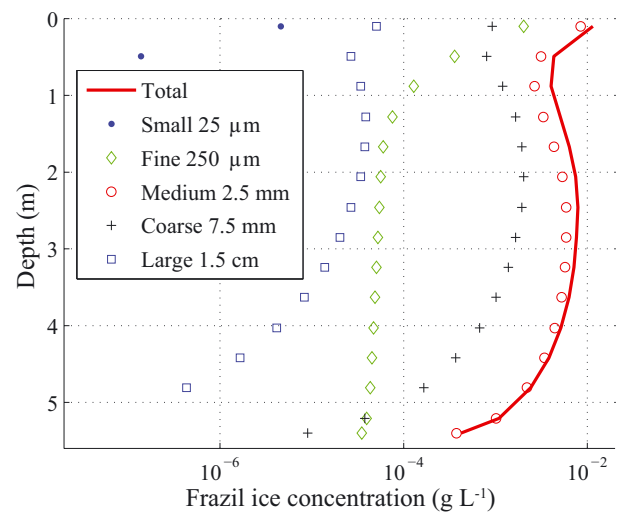


Fig. 7. The modeled concentration of frazil ice at 1500 h on 1 April. The frazil ice concentration reaches a semi-steady state at ~ 1200 h, and remains very similar throughout the 24 hour model run.

crucial processes in homogenizing the water column and in keeping it open.

An offshore drift of frazil was observed away from the ice edge during the field period (Fig. 2). This was probably due to a local offshore current in the surface set up by the wind, as calculated by the model. In this way, the open water was continuously exposed to the cold atmosphere. Furthermore, the offshore frazil drift probably limited the local frazil-ice growth, by continuously removing crystals that otherwise would grow in the supercooled water. Model runs without offshore frazil advection resulted in higher frazil concentrations, but lower supercooling than measured (not shown). The decrease in temperature towards the surface (Fig. 3) is consistent with an upward heat flux driven by the colder atmosphere, and controls the increasing supercooling towards the surface (Fig. 6), as the salinity barely increases towards the surface above 4 m depth. The colder and barely saltier surface layer creates a slightly unstable water column for the upper 4 m (Fig. 3) and indicates ongoing convection, driven from the surface.

Growing frazil ice releases brine. With the strongest supercooling occurring at the surface, the largest brine release should take place there. As the salinity is nearly homogeneous down to 3 m depth (Fig. 3), the ongoing convection is likely to be strong enough to mix the released brine downward. The model salinity (not shown) is also very homogeneous, but increases over the 24 hour model run. This points to one of the limitations of the one-dimensional model approach, that it is unable to properly account for advection of temperature and salinity into the model column. Model results indicate a compensating onshore flow in the lower layer between 2.0 and 5.0 m. An advection like this would bring water from the deeper polynya further offshore. The CTD profile in Figure 3 may well support this, showing a layer below 4 m depth with increasing temperature and salinity towards the bottom. This inflowing water is probably influenced by convective plumes over a wider area increasing the salinity slightly, but being less supercooled.

Given that there are no observations of current and the field site was in shallow water at the fast ice edge, there are

other possible explanations for the observed supercooling. Fast ice with significant deformation could produce brine that drains in plumes and forms stalactites reaching the bottom. Such stalactites could form because the brine would be below the freezing point of ambient sea water, and lead the brine systematically down to the bottom without further mixing. Supercooling could then occur due to the higher molecular diffusion of heat than salt between the cold, saline bottom plume and water above. Such a mechanism could also occur around more normal convective plumes in shallow water, in which case the largest supercooling should be found at depths close to the bottom.

Here, we reject this alternative process, based on the CTD data showing a well-mixed water column (Fig. 3). The model results also reproduce the measured level of supercooling, both at the surface and at the bottom. The CTD profiles taken through the fast ice (location FI) also show less supercooling overall than the profiles taken in the open water at the fast ice edge (location PY), as seen in Figure 6, indicating that open-water heat flux was the dominant forcing. Strong tidal currents, predominately flowing alongshore, help mix the shallow water column efficiently and downplay the effects of molecular diffusion.

The water column in the polynya gradually changed from being very saline and strongly in situ supercooled to less saline and then above freezing point during the measuring period (Fig. 4). This indicates a change of water mass inside the polynya, and Figure 5 shows that this is related to the wind direction on Hopen. Model simulations show that easterly winds result in a northward Ekman transport in Storfjorden (Skogseth and others, 2007). Further, observations in late April 2006 indicate a north–south density gradient across the fjord mouth with less saline and warmer water outside the sill (Skogseth and others, 2008). The wind direction on Hopen changed from northeast, with cold air, to east, with gradually warmer air. At the same time, the net heat flux decreased towards zero (Fig. 5a and b). The water column became warmer than the freezing point and less saline (Fig. 5c), indicating a gradual replacement of the supercooled and saline water mass with less cold and saline water from south of Storfjorden.

The brine release associated with the frazil ice formation in supercooled water gradually transformed the polynya water into brine-enriched shelf water (BSW) (Skogseth and others, 2005b), which flows down to the deeper parts of Storfjorden (Skogseth and others, 2008). When the Storfjorden basin is filled to sill level, the BSW overflows the sill as a bottom current towards the West Spitsbergen Shelf (Schauer, 1995; Schauer and Fahrback, 1999; Fer and others, 2003, 2004; Skogseth and others, 2005a,b, 2008). Then it descends the shelf break to depths with similar density as it continues into the Fram Strait (Quadfasel and others, 1988; Jungclaus and others, 1995; Skogseth and others, 2005a) and is hence a source to intermediate and deep water in the Arctic Ocean. A separate paper (Skogseth and others, 2008) contains much of the onward consequences of the BSW production, water mass transformation, downflow of dense brine water and interannual variability. Herein, we focus on the supercooling process itself, as we think it should be of general interest outside the oceanographic community.

Real or false supercooling?

The supercooling of $0.037 \pm 0.005^\circ\text{C}$ observed directly in the Storfjorden polynya with frazil-ice growth (Fig. 5d)

is the strongest observed Arctic supercooling in recent years. Compared to the supercooling of 0.13°C reported by Coachman (1966), our observations are more reliable, due to improved instrument accuracy and determination of the freezing-point temperature (Millero, 1978). Further, our observations are corrected with accompanying water samples and within the expected degree of supercooling from laboratory experiments (Daly, 1984; Smedsrud, 2001). However, to make 'real' measurements of supercooling is difficult, and we have to discuss several aspects of the measurements related to the ice-formation process that the supercooling is intimately connected to. To the extent it is possible, we have excluded the possibility of an over-estimation of the supercooling level caused by false (too low) conductivity measurements due to frazil ice, or other ice formation inside the instrument cell as discussed below.

Significant volumes of ice inside a conductivity cell will lower the conductivity measurement. This would falsely indicate a fresher water mass with a higher freezing point, and the correctly measured temperature would therefore artificially seem supercooled. The CTD was stored in a heated instrument box that kept the sensors warm enough to avoid these problems during normal deployment in Arctic waters. The conductivity sensor on the SBE19 instrument could clog when ~ 5 mm crystals entered and were unable to exit, but this would give very low and easily detectable salinity values. Slightly smaller crystals would give spikes towards lower values. Through our careful analysis of the data together with the calibration experts at SeaBird, we have not seen such spikes in the raw data recorded at 2 Hz.

Another possible source of error could be a thin film around the conductivity cell. Such a film would produce stable 'lower than real' measurements, but would also impose a steady drift towards lower salinities. Such drift was not detected in the data. Overall the conductivity and salinity were stable throughout each deployment, and no systematic lowering could be found.

From being on the ice, our impression was that most of the frazil was advected away from the fast ice we were standing on. This corresponds qualitatively with the model results shown in Figure 7, indicating maximum concentrations of frazil of 0.012 g L^{-1} , consisting mostly of crystals 2.5 mm in diameter. The few samples of frazil that we could take were from a small bay made by a grounded iceberg at the fast ice edge. This small bay collected some frazil as the iceberg blocked the surface drift. Frazil crystals are small, and no instruments exist to measure frazil concentration or size accurately.

The surface water samples were drawn taking care to exclude any visible frazil crystals in the bottles. However, collecting these water samples in a cold and windy atmosphere is not straightforward. Immediate freezing occurs inside the bottles unless they are sufficiently heated, and water droplets and snow prevent clear visibility of the bottles.

Given the model results above, some volume of frazil crystals must be allowed in the water samples. If the measured supercooling of 0.037°C was completely artificial, the 'real' surface salinity should be 36.11 psu, that is 0.63 psu higher than the measured value of 35.48 psu. This would then imply a freezing point of -1.986°C , which is close to the measured temperature in Figure 4. The frazil volume needed to offset the salinity with 0.63 psu is as high as 18 g L^{-1} . In a 2 dL bottle this is almost 4 g, and should have been clearly

visible. It is also three orders of magnitude larger than the modeled frazil concentration of 0.01 g L^{-1} (Fig. 7).

During our careful reprocessing of the data after calibration, we found that the largest supercooling occurred around 1511 h on 1 April (Fig. 5d). This was caused by the lower temperature at 1 m depth compared to that at 5 m, which was $\sim 0.025^\circ\text{C}$ higher. The salinity was ~ 0.02 psu higher near the surface than at the bottom, as we would expect from an unstable water column having salt added from freezing most efficiently close to the surface. This had an insignificant influence on the freezing point, $\sim 0.001^\circ\text{C}$. Conclusively, this implies that even if the supercooling at 5 m depth was offset by frazil ice (too low), the temperature could clearly not be higher than the freezing point. Given the well-mixed water column, a $\sim 0.025^\circ\text{C}$ colder surface layer had to be at least 0.025°C supercooled. This is confirmed by the model (Fig. 6) and follows expectations of a strong upward heat flux. The model thus confirms the physical relation between a large heat flux, small concentrations of frazil ice and a large supercooling. It also confirms the measured vertical temperature difference at the fast ice edge being $\sim 0.020^\circ\text{C}$ from the 12 CTD profiles made between 1510 and 1513 h on 1 April (Fig. 5d).

The maximum salinity offset from frazil ice in the surface bottle sample could not have been larger than 0.17 psu without increasing the temperature above the freezing point at 5 m depth. This implies that $\sim 5 \text{ g L}^{-1}$ homogeneous volume concentration of pure frazil crystals would lower the 'real' supercooling, compared to that observed, by 0.010°C . This remains a theoretical possibility given the practical difficulty of sampling water under such windy and cold conditions. However, given the model's reproduction of the gradient in temperature and reasonable values of the other qualitative validations, we find that the most likely error in supercooling caused by the presence of frazil ice in the conductivity cell and the water samples was smaller than the calibration uncertainties of $\pm 0.005^\circ\text{C}$. Frazil ice was probably present, but with concentrations below $\sim 0.02 \text{ g L}^{-1}$, as indicated by the model. This would lower the 'real' salinity by < 0.001 psu, corresponding to a correction of the freezing point of less than $\sim 0.0001^\circ\text{C}$, far below the instrument and calibration uncertainties.

Supercooling sensitivity to frazil crystals

The model sensitivity to supercooling as a function of available crystals at the surface (snow) was tested. Increasing the snow from 0.07 mm d^{-1} in the normal model run to 0.7 mm d^{-1} lowered the supercooling at the surface to $0.005\text{--}0.010^\circ\text{C}$. No supercooling was calculated at the bottom, and the temperature gradient was small. Less snow, 0.007 mm d^{-1} , increased the supercooling to 0.090°C . The supercooling became very homogeneous with depth and was clearly overestimated.

Using only large snow crystals made the supercooling increase steadily with time, to reach 0.700°C at 24 hours. This is clearly unrealistic and points to the fact that small crystals are probably generally available to start the frazil growth process. Large frazil crystals grow slowly (Smedsrud and Jenkins, 2004). Using only small crystals in the snow created a maximum supercooling similar to that measured, $\sim 0.035^\circ\text{C}$. The steady supercooling solution decreased to 0.020°C at the surface and 0.010°C at the bottom. This is quite similar to the normal run shown in Figure 6, but the supercooling is too small in the lower layer. This indicates

that the large crystals do not contribute much to the frazil growth process when there are small crystals present. Large crystals are buoyant, rise effectively and are advected away without participating actively in the growth process.

This analysis of sensitivity tells us that the level of supercooling may be quite dependent on the properties of the snowdrift or snowfall. As direct in situ observations from polynyas are sparse, it remains conjectural whether or not higher levels of supercooling may be documented in the future. Our impression from the field is that in wind-driven polynyas there is always snowdrift, and small water droplets being thrown up in the air that freeze. These will start frazil-ice growth to some extent. With stronger winds, a larger snowdrift will probably occur. Thus, the maximum level of supercooling should occur in a polynya with the highest possible heat flux, with a fairly moderate wind forcing and no snowfall. This would also create moderate snowdrift, and perhaps higher levels of supercooling than we have documented here.

Frazil-ice growth and brine release

The large heat flux, up to 400 W m^{-2} (Fig. 5b), resulted in a substantial formation of frazil ice ($\sim 50 \text{ kg m}^{-2} \text{ d}^{-1}$; Table 2). As the frazil crystals are fresh water, the integrated heat-flux estimates are equal to 0.16 m of fresh ice during the 3 days with observed supercooling. This fresh-ice volume has lost all its salt (5.5 kg m^{-2}) to the water column it grew in. Using the maximum observed salinity of 35.7 psu on 31 March (Fig. 5c), the accumulated frazil-ice growth during the 3 days of supercooling would increase the salinity of the 5 m water column by 1.2 psu, if distributed evenly.

The grown volume of frazil forms an upper layer of grease ice, a slurry of $\sim 25\%$ pure frazil ice and $\sim 75\%$ sea water (Martin and Kauffman, 1981). From a small number of field grease-ice samples, the mean fresh frazil ice concentration was found to be 25.3% (Smedsrud and Skogseth, 2006). Using this value implies that for an observer, a bulk sample of this grease ice would be $0.16 \text{ m}/0.253 = 0.63 \text{ m}$, and have bulk salinities around 25 psu. Seven such samples were taken in a small enclosed bay along the polynya edge, where the grease did not drift away. The samples were taken following Smedsrud and Skogseth (2006) on 2 and 3 April, and gave a mean salinity of 26.2 psu, the range being 23.2–28.8 psu.

As frazil crystals grow, brine is released to the surrounding water. From laboratory experiments, Ushio and Wakatsuchi (1993) concluded that this brine releases from the accumulated frazil ice at the surface, as well as from individual crystals in suspension. Field data from the drained water from the grease ice indicate that the brine salinity increases to ~ 1 psu above that of the surrounding surface water (Smedsrud and Skogseth, 2006). It can therefore be assumed that all the brine drains from the grease ice within a relatively short time-frame. One would then expect to see a 1.2 psu increase in salinity in the 5 m water column during fieldwork, but this is not the case. Instead, the observed salinity of the water column decreased by 0.34 psu during the supercooling event (Fig. 5c). This can only be caused by water mass replacement.

During winter, frazil-ice growth and accompanying brine release gradually increase the salinity of the polynya water that eventually transforms to cold and saline BSW (Skogseth and others, 2005a). Subsequent downflow of BSW from the shallow polynya area to the deeper part of Storfjorden was observed on 6 April 2006 (Skogseth and others, 2008), only 4 days after the last observed supercooling (Fig. 5c). At

the measuring site, the salinity started to decrease before temperature increased, probably as a result of BSW being replaced by a supercooled but less saline water mass when the downflow of BSW from the shallow shelves occurred.

CONCLUSIONS

Cold northeasterly winds created a large polynya in Storfjorden for several days in April 2006, resulting in a very homogeneous, saline and supercooled nearshore water column. The supercooling was driven by offshore wind and surface heat flux up to 400 W m^{-2} that lasted until the wind direction turned to the east, bringing in warmer air masses and warmer, less saline water from the south. Frazil ice formed at the surface and was transported downwind, but seven surface frazil/grease ice samples were taken from a small enclosed bay along the upwind polynya edge. The mean grease-ice salinity of 26.2 psu supports earlier estimates of ~25% fresh ice and ~75% sea water in the surface grease-ice layer.

The maximum in situ supercooling observed was $0.037 \pm 0.005^\circ\text{C}$ during the end of the polynya event. The supercooling was stronger (0.020°C) at the surface than at the bottom, clearly confirming a strong surface heat flux. This heat flux drove frazil formation, as confirmed by model results, and the measured supercooling level was well reproduced.

The possible presence of small (not visible) frazil crystals homogeneously distributed in the water column was considered as a possible error of the high supercooling. As the modeled concentration of frazil ice was lower than 0.02 g L^{-1} , this effect changes the corresponding freezing point ($\pm 0.001^\circ\text{C}$) less than the instrument uncertainty ($\pm 0.005^\circ\text{C}$). If the frazil concentration was an order of magnitude larger, but still not visible, a small theoretical possibility remains that the 'real' maximum supercooling may be lowered by 0.010°C . The 'real' maximum supercooling measured was certainly not lower than 0.027°C .

To our knowledge, this is the first in situ supercooling observed in an Arctic polynya with concurrent hydrographic sampling and direct observations of frazil-ice growth. This is also the strongest observed supercooling in the Arctic in recent years with improved instrument accuracy. Supercooling at the levels presented here is probably of general occurrence in any wind-driven coastal polynya that experiences such cooling rates and has a homogeneous water mass at the freezing point. These conditions are certainly present in the Storfjorden polynya, and we suggest this as a key area to conduct future supercooling studies.

ACKNOWLEDGEMENTS

This work was conducted as a part of the Polar Ocean Climate Processes project (PROCLIM) funded by the Norwegian Research Council through grant 155923/700, and the International Polar Year project Bipolar Atlantic Thermohaline Circulation (BIAC) through grant 176082/S30. We thank the logistic department at UNIS, the Governor of Svalbard and Airlift AS for support and service. We are grateful to S. Claes and J. Jeppesen for help during the fieldwork. C. Janzen at SeaBird Electronics is acknowledged for her service on the CTD calibration. This is publication A205 from the Bjerknnes Centre for Climate Research.

REFERENCES

- Coachman, L.K. 1966. Production of supercooled water during sea ice formation. *In Proceedings of the Symposium on the Arctic Heat Budget and Atmospheric Circulation, Lake Arrowhead, California, 31 January–4 February 1966*. Santa Monica, CA, The Rand Corporation, 497–529.
- Countryman, K.A. 1970. An explanation of supercooled waters in the Ross Sea. *Deep-Sea Res.*, **17**, 85–90.
- Daly, S.F. 1984. Frazil ice dynamics. *CRREL Monogr.* 84-1.
- Drucker, R., S. Martin and R. Moritz. 2003. Observations of ice thickness and frazil ice in the St Lawrence Island polynya from satellite imagery, upward looking sonar, and salinity/temperature moorings. *J. Geophys. Res.*, **108**(C5), 3149. (10.1029/2001JC001213.)
- Fer, I., R. Skogseth, P.M. Haugan and P. Jaccard. 2003. Observations of the Storfjorden overflow. *Deep-Sea Res. I*, **50**(10–11), 1283–1303.
- Fer, I., R. Skogseth and P.M. Haugan. 2004. Mixing of the Storfjorden overflow (Svalbard Archipelago) inferred from density overturns. *J. Geophys. Res.*, **109**(C1), C01005. (10.1029/2003JC001968.)
- Fofonoff, N.P. and R.C. Millard, Jr. 1983. Algorithms for computation of fundamental properties of seawater. *UNESCO Tech. Pap. Mar. Sci.* 44.
- Haarpaintner, J., J. Gascard and P.M. Haugan. 2001. Ice production and brine formation in Storfjorden, Svalbard. *J. Geophys. Res.*, **106**(C7), 14,001–14,014.
- Jungclauss, J.H., J.O. Backhaus and H. Fohrmann. 1995. Outflow of dense water from the Storfjord in Svalbard: a numerical model study. *J. Geophys. Res.*, **100**(C12), 24,719–24,728.
- Khazendar, A. and A. Jenkins. 2003. A model of marine ice formation within Antarctic ice shelf rifts. *J. Geophys. Res.*, **108**(C7), 3235. (10.1029/2002JC001673.)
- Kivisild, H.R. 1970. River and lake ice terminology. *In Proceedings of the IAHS Symposium on Ice and its Action on Hydraulic Structures, 7–10 September 1970, Reykjavík, Iceland*. Reykjavík, International Association for Hydraulic Research, 1–14.
- Leonard, G.H., C.R. Purdie, P.J. Langhorne, T.G. Haskell, M.J.M. Williams and R.D. Frew. 2006. Observations of platelet ice growth and oceanographic conditions during the winter of 2003 in McMurdo Sound, Antarctica. *J. Geophys. Res.*, **111**(C4), C04012. (10.1029/2005JC002952.)
- Lewis, E.L. and R.G. Perkin. 1983. Supercooling and energy exchange near the Arctic Ocean surface. *J. Geophys. Res.*, **88**(C12), 7681–7685.
- Lewis, E.L. and R.G. Perkin. 1986. Ice pumps and their rates. *J. Geophys. Res.*, **91**(C10), 11,756–11,762.
- Littlepage, J.L. 1965. Oceanographic investigations in McMurdo Sound, Antarctica. *In Llano, G.A., ed. Biology of the Antarctic seas II*. Washington, DC, American Geophysical Union, 1–37. (Antarctic Research Series 5.)
- Lusquiños, A.J. 1963. Extreme temperatures in the Weddell Sea. *Univ. Bergen Årb. Mat. Naturv. Ser.* 23.
- Martin, S. 1981. Frazil ice in rivers and oceans. *Annu. Rev. Fluid Mech.*, **13**, 379–397.
- Martin, S. and P. Kauffman. 1981. A field and laboratory study of wave damping by grease ice. *J. Glaciol.*, **27**(96), 283–313.
- Mellor, G.L. and T. Yamada. 1982. Development of a turbulent closure model for geophysical fluid problems. *Rev. Geophys. Space Phys.*, **20**(4), 851–875.
- Millero, F.J. 1978. Freezing point of sea water. *UNESCO Tech. Pap. Mar. Sci.* 28, 29–35.
- Nicholls, K.W., K. Makinson and S. Østerhus. 2004. Circulation and water masses beneath the northern Ronne Ice Shelf, Antarctica. *J. Geophys. Res.*, **109**(C12), C12017. (10.1029/2004JC002302.)
- Omstedt, A. and U. Svensson. 1984. Modeling supercooling and ice formation in a turbulent Ekman layer. *J. Geophys. Res.*, **89**(C1), 735–744.

- Orheim, O., J.O. Hagen, and A.C. Sætrang. 1990. Glaciologic and oceanographic studies on Fimbulisen during NARE 1989/90. *FRISP Rep.* 4, 120–131.
- Quadfasel D., B. Rudels and K. Kurz. 1988. Outflow of dense water from Svalbard Fjord into the Fram Strait. *Deep-Sea Res.*, **35**(7), 1143–1150.
- Schauer, U. 1995. The release of brine-enriched shelf water from Storfjord into the Norwegian Sea. *J. Geophys. Res.*, **100**(C8), 16,015–16,028.
- Schauer, U. and E. Fahrbach. 1999. A dense bottom water plume in the western Barents Sea: downstream modification and interannual variability. *Deep-Sea Res.* **146**(12), 2095–2108.
- Shcherbina, A.Y., L.D. Talley and D.L. Rudnick. 2004. Dense water formation on the northwestern shelf of the Okhotsk Sea: 1. Direct observations of brine rejection. *J. Geophys. Res.*, **109**(C9), C09S08. (10.1029/2003JC002196.)
- Sherwood, C.R. 2000. Numerical model of frazil-ice and suspended-sediment concentrations, and formation of sediment-laden ice in the Kara Sea. *J. Geophys. Res.*, **105**(C6), 14,061–14,080.
- Skogseth, R., P.M. Haugan and J. Haarpaintner. 2004. Ice and brine production in Storfjorden from four winters of satellite and in situ observations and modeling. *J. Geophys. Res.*, **109**(C10), C10008. (10.1029/2004JC002384.)
- Skogseth, R., I. Fer and P.M. Haugan. 2005a. Dense-water production and overflow from an arctic coastal polynya in Storfjorden. In Drange, H., T. Dokken, T. Furevik, R. Gerdes and W. Berger, eds. *The Nordic seas: an integrated perspective – oceanography, climatology, biogeochemistry, and modeling*. Washington, DC, American Geophysical Union, 73–88. (Geophysical Monograph 158.)
- Skogseth, R., P.M. Haugan and M. Jakobsson. 2005b. Watermass transformations in Storfjorden. *Continental Shelf Res.*, **25**(5–6), 667–695.
- Skogseth, R., A.D. Sandvik and L. Asplin. 2007. Wind and tidal forcing on the meso-scale circulation in Storfjorden, Svalbard. *Continental Shelf Res.*, **27**(2), 208–227.
- Skogseth, R., L.H. Smedsrud, F. Nilsen and I. Fer. 2008. Observations of hydrography and downflow of brine-enriched shelf water in the Storfjorden polynya. *J. Geophys. Res.*, **113**(C8), C08049. (10.1029/2007JC004452.)
- Smedsrud, L.H. 2001. Frazil-ice entrainment of sediment: large-tank laboratory experiments. *J. Glaciol.* **47**(158), 461–471.
- Smedsrud, L.H. 2002. A model for entrainment of sediment into sea ice by aggregation between frazil-ice crystals and sediment grains. *J. Glaciol.*, **48**(160), 51–61.
- Smedsrud, L.H. and A. Jenkins. 2004. Frazil ice formation in an ice shelf water plume. *J. Geophys. Res.*, **109**(C3), C03025. (10.1029/2003JC001851.)
- Smedsrud, L.H. and R. Skogseth. 2006. Field measurements of Arctic grease ice properties and processes. *Cold Reg. Sci. Technol.*, **44**(3), 171–183.
- Untersteiner, N. and R. Sommerfeld. 1964. Supercooled water and the bottom topography of floating ice. *J. Geophys. Res.*, **69**(6), 1057–1062.
- Ushio, S. and M. Wakatsuchi. 1993. A laboratory study on supercooling and frazil ice production processes in winter coastal polynyas. *J. Geophys. Res.*, **98**(C11), 20,321–20,328.

MS received 9 October 2007 and accepted in revised form 8 November 2008